Available online at www.sciencedirect.com
SCIENCE DIRECT
Polymer 47 (2006) 2483–2492
polymer
www.elsevier.com/locate/polymer

Single molecule force spectroscopy of smart poly(ferrocenylsilane) macromolecules: Towards highly controlled redox-driven single chain motors

Shan Zou, Igor Korczagin, Mark A. Hempenius, Holger Schönherr, G. Julius Vancso *

Materials Science and Technology of Polymers, MESA+ Institute for Nanotechnology, University of Twente, P.O. Box 217, Enschede 7500 AE, The Netherlands

Received 6 October 2005; received in revised form 6 December 2005; accepted 8 December 2005
Available online 13 February 2006

Abstract

We investigated various stimuli-responsive poly(ferrocenylsilane) (PFS) polymers as model systems for the realization of molecular motors powered by a redox process. Covalently end-grafted PFS on gold, as well as PFS homopolymers and block copolymers in ultrathin films, were studied by AFM-based single molecule force spectroscopy (SMFS). Surface confined PFS macromolecules were chemically oxidized by addition of tetracyanoethylene or were completely and reversibly oxidized (and reduced) in situ by applying an electrochemical potential. Chemical oxidation was successful only for the block copolymers. The entropic elasticity of neutral PFS chains (Kuhn length $I_K \sim 0.40$ nm) was found to be larger than that of oxidized PFS chains ($I_K \sim 0.65$ nm) in the lower force regime. The elasticities could be reversibly controlled in situ by adjusting the applied potential in electrochemical SMFS experiments. For a single PFS macromolecule (DP = 80) operating cycle, a work output and an efficiency of 3.4×10^{-19} J and $\sim 5\%$, respectively, were estimated based on the single chain experimental data.

Keywords: Atomic force microscopy; Electrochemistry; Stimuli-responsive polymer

1. Introduction

In nature a plethora of molecular, including rotary and flagellar, motors can be found, which perform specific functions, such as transport of cargo and translocation. Important examples are, among others, ATP synthase [1–3], kinesine [4], myosin [5], and flagellar motors [6] in bacteria, respectively. In general, there are different forms of energy that can be used to power these motors, such as, e.g. light, redox or chemical energy.

Inspired by these naturally occurring motors that have been optimized in the process of evolution a large variety of artificial or synthetic motors has been designed. These synthetic molecular motors comprise molecular switches, shuttles, scissors, rotating modules and muscles [7–13]. Recently, studies of artificial molecular motors at the single molecule level have become possible, thus opening a new area for research aimed at obtaining a fundamental understanding of the relevant molecular scale processes on the one hand and at realizing and exploiting the smallest man-made, artificial machinery on the other hand.

The most efficient thermal engine with an ideal gas is the Carnot cycle [14]. The amount of the work (W_{out}) produced by the system is equal to the net heat transferred during the processes. The efficiency of the cycle, η, is defined as the amount of the work produced by the system divided by the supplied heat (heat-in). In electrochemistry, isothermal chemical cycles are known to yield more (electrical) work from the oxidation of chemicals than the work that is accessible from thermal cycles (where the same chemicals are burned in order to create the high temperature reservoir) [15].

A direct coupling between the change of chemical free energy and the production of mechanical work can be obtained by employing a macromolecular working substance [16]. This has been demonstrated for the cyclic operation of a cross-linked collagen tape between a reservoir of high chemical potential and one of low chemical potential [17]. This isothermal, chemical cycle of collagen derives its power from the isothermal transport of salt and water from high to low chemical potential, just as the thermal cycle derives its power from the transport of entropy from high to low temperature.

To provide direct coupling between changes in chemical free energy and the production of mechanical work (see above)

* Corresponding author. Tel.: +31 53 489 2967; fax: +31 53 489 3823.
E-mail address: g.j.vancso@tnw.utwente.nl (G.J. Vancso).

0032-3861/$ - see front matter © 2006 Elsevier Ltd. All rights reserved.
doi:10.1016/j.polymer.2005.12.091

and to afford sufficiently large responses to external stimulation, stimuli-responsive polymers have attracted growing attention. As proposed more than a decade ago [18] and also demonstrated for macroscopic model actuators [19–21], electric fields (surface charges), pH changes, temperature changes, or changes of the redox state, among other stimuli, have been used for excitation.

These concepts have only been recently successfully extended to the single molecule scale in the attempt to mimic the naturally occurring molecular motors. The group of Gaub reported on a polymer comprising azobenzene units along the main chain, which was stretched and contracted by an externally applied stimulus, i.e. light [22]. Switching between the *trans*- and *cis*-azobenzene isomers could selectively change the contour length of the polymer chain, as detected by atomic force microscopy (AFM)-based approaches on individual molecules. In principle this chain could perform work and may also serve as a model for a single macromolecule-based motor. The corresponding AFM measurements, also called single molecule force spectroscopy (SMFS), are based on the measurement of mechanical forces on the single molecule level. As has been reviewed recently [23–25], mechanical experiments with single macromolecules have been carried out by AFM to directly probe subtle differences in polymer chain conformational changes. Conformational transitions, such as for instance force-induced chair-to-boat transitions in polysaccharides, have been widely investigated, and the mechanical manipulation of single pyranose rings has been achieved [26–29]. SMFS and related very sensitive force measurements, including force clamp techniques (see, e.g. Ref. [30]), have proven to be a successful strategy to address and probe single functional molecules and thus nanometer-sized devices with macroscopic instrumentation [31,32]. For this interfacing with the macroscopic world also appropriate immobilization schemes and surface modification procedures are essential.

In view of future applications and utilization of single molecule motors, high density arrays, in which these motors can be addressed individually, appear to be necessary. The concomitant intermolecular distances would likely also be on molecular length scales. Thus, optical means would be limited to near-field optical approaches, while many other stimuli mentioned, such as pH or temperature changes in solution, appear unfeasible given typical diffusion lengths of the active species and temperature diffusion, respectively. However, redox-driven processes, as also known from a multitude of biologically highly relevant processes, seem to be advantageous in combination with, for instance, advanced nanoelectrode fabrication [33].

In the context of single macromolecular motors, redox chemistry induced elasticity changes in organometallic polymers [34–36], as well as pH sensitive macromolecules, were investigated more recently [37]. In both approaches the essential component of designing a molecular motor has been implemented, i.e. the systems allow for a change of the conformational or chemical state of the macromolecule resulting in the reversible control of the elasticity of the polymer chain (before and after stimulation).

The mentioned redox chemistry-based stimuli-responsive system is based on polyferrocenylsilane (PFS) macromolecules. These polymers, which are composed of alternating ferrocene and alkylsilane units in the main chain [38–41], are interesting in the very context of molecular motors owing to the possibility of reversible oxidation and reduction of ferrocenyl groups along a given polymer chain (Scheme 1) [42–44].

In this paper, we report on the systematic investigation of a redox chemistry-based stimulus for tuning the elasticity of individual stimuli-responsive PFS polymer chains in an attempt to realize a single (macro)molecular motor. In addition to the demonstration of the feasibility of a motor consisting of one single PFS macromolecule, we compare electrochemically and chemically triggered single molecule responses.

2. Experimental section

2.1. Materials

Ethylene sulfide end-capped poly(ferrocenyldimethylsilane) $(PFS)_{100}$, PFS homopolymer (PFS_{homo}), and poly(styrene-*block*-ferrocenyldimethylsilane) (PS-*b*-PFS) (all synthesized by anionic polymerization) were available from other studies [44–46]. The following molar mass data were determined by GPC in THF, relative to polystyrene standards: PFS_{100} (M_n = 22,600 g/mol, DP_n = 92, M_w/M_n = 1.13), PFS_{homo} (M_n = 71,670 g/mol, M_w = 75,420 g/mol, M_w/M_n = 1.05), PS-*b*-PFS (M_n = 77,680 g/mol, M_w = 78,440 g/mol, M_w/M_n = 1.01, 22.8% (by mass), 19.8% (by volume) ferrocenyl groups). Polystyrene standards (M_w = 20,650 g/mol, M_w/M_n = 1.03; M_w = 79,000, M_w/M_n = 1.16) were used for the SMFS blank experiments.

The PFS polymers were chemically oxidized using tetracyanoethylene (TCNE) in CH_2Cl_2 at RT with equal mole fraction to ferrocenyl groups until the color of the solution became dark green.

2.2. Substrates and samples

(a) Gold substrates (11 × 11 mm^2, 250 nm Au on 2 nm Cr on borosilicate glass) for electrochemical SMFS measurements were purchased from Metallhandel Schröer GmbH (Lienen, Germany). Au(111) samples were obtained by annealing these substrates in a high purity H_2 flame for 5 min [47]. PFS_{100} layers were prepared by self-assembly from dilute toluene solutions (conc. ~ 0.005 mg/L) following the standard procedures discussed in Refs. [44,45]. PFS_{homo} thin layers were prepared by spin-coating a dilute toluene solution (~0.005 mg/L) on Au(111) substrates.

(b) PFS films were also spin-coated from toluene solution (~0.005 mg/mL) onto silicon wafers; film thicknesses (<10 nm) were determined with a Plasmos SD 2002 ellipsometer using a wavelength of 632.8 nm (refractive index = 1.687) [45]. Prior to use, all these substrates were cleaned in piranha solution (7:3 H_2SO_4:H_2O_2 (30%) by volume), then rinsed with Milli-Q water and ethanol and dried in a nitrogen stream. Caution: piranha solution

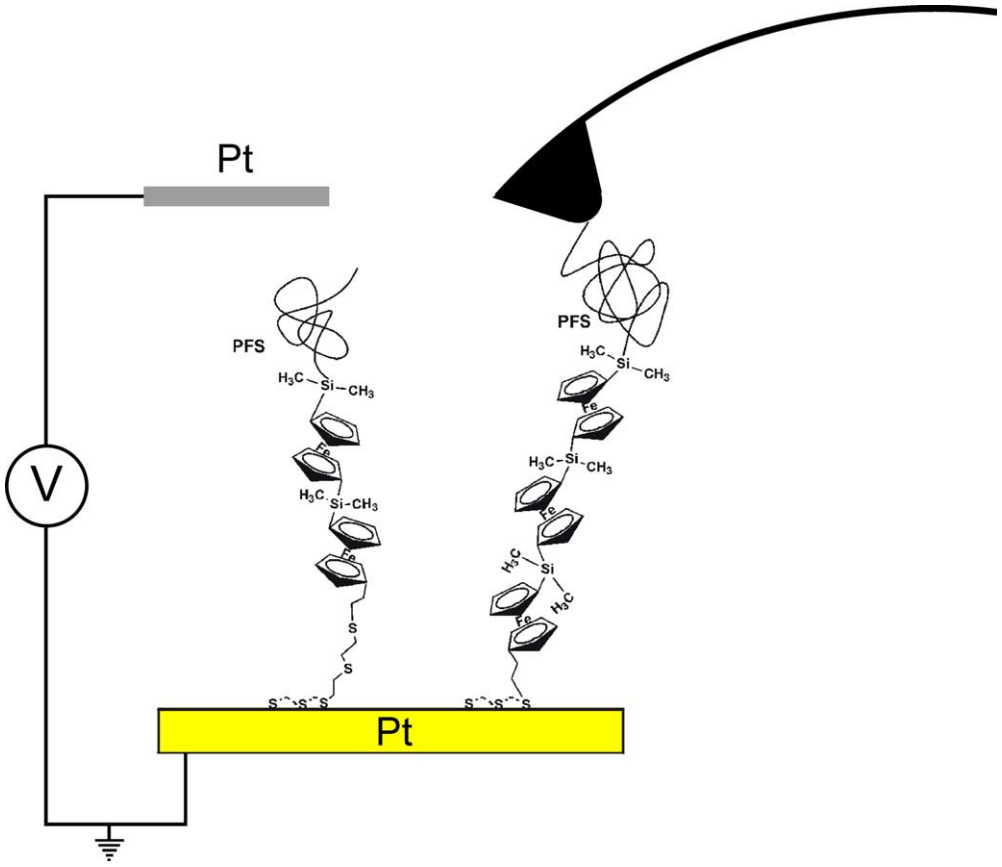

Scheme 1. Schematic illustration of stretching stimuli-responsive single PFS_{100} polymer chains using electrochemical AFM-based SMFS. Similarly, the oxidation and reduction could be induced chemically by adding oxidants and reducing agents, respectively.

should be handled with extreme caution: it has been reported to detonate unexpectedly.

2.3. Force measurements

Force spectroscopy experiments were performed by in situ AFM in liquid environment with a NanoScope IIIa multimode AFM (Veeco/Digital Instruments (DI), Santa Barbara, CA) fitted with either a normal DI liquid cell or DI electrochemical liquid cell (volume in each case $\sim$50 μL). Commercially available V-shaped Si_3N_4 cantilevers (model NP, Veeco/DI) were used. Each cantilever was calibrated after a given experiment according to the equipartition method, by measuring the thermal excitation of the tip to compute its spring constant [48,49]. The measured spring constants of the cantilevers varied between 0.075 and 0.105($\pm$0.017) N/m.

For electrochemical SMFS experiments, a DI electrochemical liquid cell equipped with an external Autolab PGSTAT10 potentiostat (ECOCHEMIE, Utrecht, The Netherlands) was used. The polymer covered gold substrate served as the working electrode; Pt wires were used as reference and counter electrodes. The electrolyte used was 0.1 M $NaClO_4$ in water. Prior to the experiments, the electrolyte was deaerated by passing nitrogen through the solution for 5 min. Cyclic voltammograms were recorded between -0.1 and $+0.5$ V_{Pt} at a scan rate of 50 mV/s. An external potential of $+0.5$ V was maintained during the force measurements to ensure the complete oxidation of PFS molecules.

3. Results and discussion

For the realization of molecular motors powered by a redox process various stimuli-responsive poly(ferrocenylsilane) polymers were investigated as model systems. The electrochemical oxidation and reduction of PFS has been studied before in the bulk [39,40,42,50] and in end-grafted PFS macromolecules on gold electrodes [45,46]. Evidence for reversible oxidation and reduction was obtained in cyclic voltammetry (CV) and differential pulse voltammetry measurements [44,45]. Chemical oxidation of PFS homopolymers, e.g. by using TNCE as oxidant, led presumably to only incomplete oxidation. PFS containing copolymers, for instance poly(styrene-*block*-ferrocenyldimethylsilanes), showed an increased solubility after chemical oxidation compared to the PFS homopolymer in organic solvents, such as THF and toluene [51]. This feature could be useful to realize sufficiently high degrees of chemical oxidation of PFS. Therefore, the elasticity of neutral, as well as chemically oxidized, single PS-*b*-PFS polymer chains was also investigated by AFM-based SMFS in addition to the end-grafted PFS_{100} molecules and PFS homopolymer, which both can be directly electrochemically addressed.

3.1. Single chain elasticity measurements on neutral PFS macromolecules

In order to compare differences of elasticity between neutral and oxidized PFS macromolecules, individual neutral PFS_{100}, PFS_{homo} and PS-*b*-PFS chains were probed by single molecule force spectroscopy. Since the targeted electrochemistry experiments were carried out in aqueous solutions, the single chain stretching of neutral PFS was studied also in aqueous solutions of $NaClO_4$.

Typical force vs. extension curves of neutral PFS_{homo} and PS-*b*-PFS chains probed in isopropanol are shown in Fig. 1 (for data of PFS_{100} stretched in alcohols, see Ref. [44]). The force–extension curves obtained from these polymers showed similar characteristics: the force value rises with the extension of the polymer chain, and drops to zero, when the rupture point is reached. Until reaching its fully extended configuration, the polymer chain exhibits no measurable conformational transitions, indicating that no detectable thermal activation barriers are overcome along the trajectory of mechanical stretching. The observation of different extension (stretching) lengths is attributed to the fact that the chains adhere via physisorption to the tip, resulting in varying position of attachment points along a given chain in different stretching experiments.

The corresponding force–extension data for neutral PFS_{100} and PFS_{homo} studied in aqueous media are shown in Fig. 2. The force–extension curves were fitted to the modified-freely jointed chain (m-FJC) model [52] (no data shown). The obtained values of Kuhn lengths I_K and segment elasticities $K_{segment}$ are shown in Table 1. The force–extension curves were also normalized by the extension that correspond to the same force value (250 pN), as shown in Figs. 1 and 2. All sets of normalized curves superimpose well, which indicates that single chains have been stretched.

From the fits of the force–extension curves, one can conclude that the extended Langevin function describes both entropic (both low and high force regime) and enthalpic (high force regime) elasticities of all types of PFS polymer chains very well. The normalized force profiles [53] of neutral PFS_{100}, PFS_{homo}, and PS-*b*-PFS in isopropanol and water, and the identical segment elasticities and Kuhn lengths for all polymer chains, respectively, confirm that individual PFS chains were stretched and the deformation of single chains of a given type under tension was measured. All PFS homopolymer chains (PFS_{100} and PFS_{homo}) possess an identical Kuhn length and segment elasticity. The parameters determined for PFS_{100} are, to within the experimental error, identical to the ones reported before for measurements in ethanol ($I_K = 0.33 \pm 0.05$ nm, $K_{segment} = 32 \pm 5$ nN/nm) [44], as well as to those of PFS_{homo}. However, the elasticity values of PS-*b*-PFS ($I_K = 0.39 \pm 0.05$ nm, $K_{segment} = 23 \pm 5$ nN/nm) differed clearly.

In order to understand the difference between elasticities obtained for homo PFS polymer and the block copolymer chains, single chain stretching experiments were carried out on polystyrene (PS) homopolymer chains in isopropanol. The fitted force–extension curves yielded a Kuhn length of 0.40 ± 0.03, and $K_{segment}$ of 18 ± 3 nN/nm. This result indicates that the lower segment elasticity of PS-*b*-PFS can be attributed to the contribution of the elasticity of the PS block.

3.2. Single chain elasticity measurements on oxidized PFS macromolecules

The ability to reversibly control the elasticity of PFS chains (neutral and oxidized) by external stimuli may be used to realize a molecular motor. After the discussion of the elastic properties of neutral PFS chains, the determination of the elastic properties of oxidized PFS chains will be treated, starting with chemical oxidation followed by electrochemical (EC) oxidation.

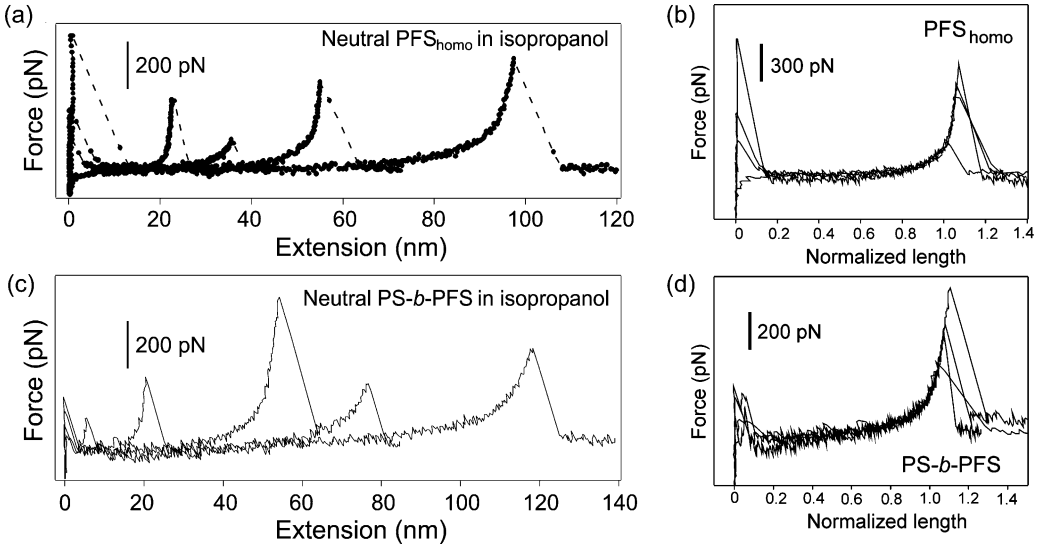

Fig. 1. (a) Force vs. extension traces of individual neutral PFS_{homo} measured in isopropanol, (b) superposition of normalized force curves for PFS_{homo}, (c) force vs. extension traces of individual neutral PS-*b*-PFS polymer chains stretched in isopropanol, and (d) superposition of normalized force curves for PS-*b*-PFS.

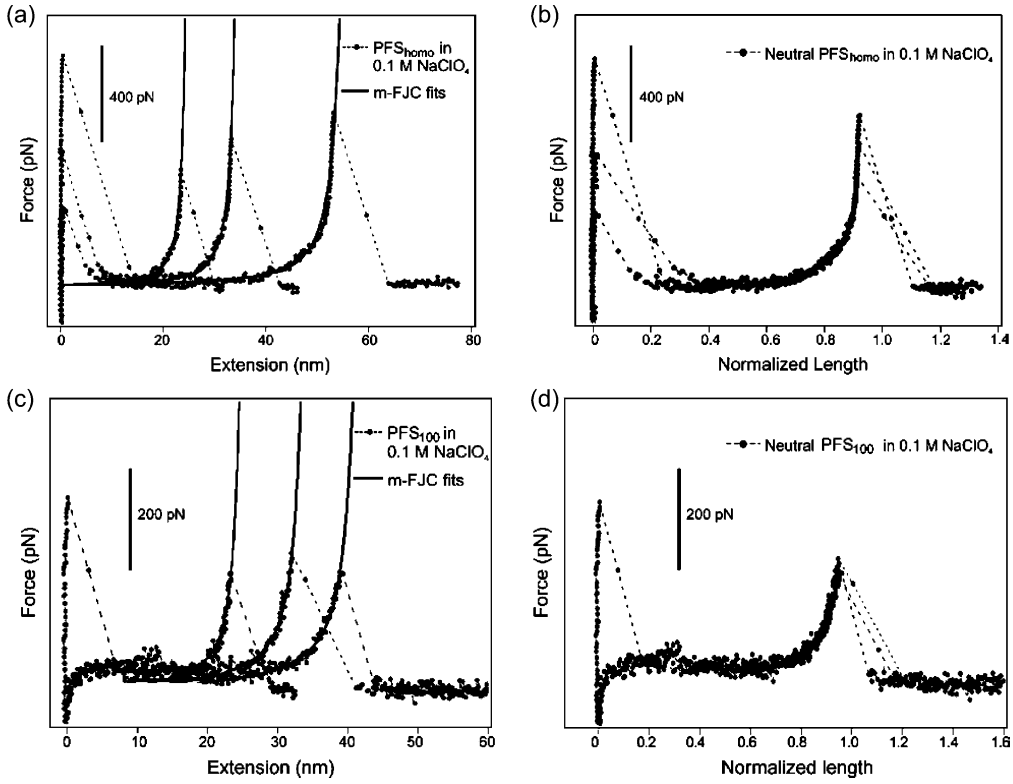

Fig. 2. (a) Force–extension curves of individual neutral PFS_{homo} polymer chains measured in 0.1M $NaClO_4$ (the solid lines represent the superimposed m-FJC fits); (b) superposition of the normalized force curves shown in (a); (c) force–extension curves individual neutral PFS_{100} chains measured in 0.1 M $NaClO_4$ (the solid lines represent the superimposed m-FJC fits); (d) superposition of the normalized force curves shown in (c). Panels (c) and (d) reproduced from Ref. [36] with permission from Wiley–VCH.

3.3. Chemically oxidized PFS macromolecules

Fig. 3 shows representative force curves obtained in SMFS experiments on PFS_{100}, PFS_{homo} and PS-*b*-PFS chains, respectively, that were subjected to conditions of chemical oxidation. To compare the force–extension relationship and the elasticity of different polymer chains with different extension lengths, the force traces were fitted with the m-FJC model and normalized by their lengths at the same given force (250 pN). Force curves of PFS_{homo} with different stretching lengths superimpose after normalization, as do the normalized force curves of PS-*b*-PFS. The superposition of normalized force curves, as well as the m-FJC fits, for PFS_{homo} and PS-*b*-PFS, respectively, indicate the elongation of individual polymer chains for both sets of data.

By contrast, the data for PFS_{homo} and PFS_{100} on one hand, and the data for PS-*b*-PFS on the other hand, clearly differ (Fig. 3(b)). Oxidized PS-*b*-PFS chains show a lower entropic elasticity compared to chemically oxidized PFS_{homo} chains, while latter ones yield identical elasticity parameters compared to the neutral PFS to within the experimental error. The corresponding Kuhn lengths and segment elasticities are shown in Table 1.

From the m-FJC fit results, shown in Table 1 for oxidized PFS with different molar mass and end-functional groups,

Table 1
Single chain elasticities of individual PFS polymer chains probed in different media in different oxidation states (data calculated from fits of force–extension data to the m-FJC model)

Solvent/condition	PFS_{100}		PFS_{homo}		PS-*b*-PFS		PS	
	I_K (nm)	$K_{segment}$ (nN/nm)	I_K (nm)	$K_{segment}$ (nN/nm)	I_K (nm)	$K_{segment}$ (nN/nm)	I_K (nm)	$K_{segment}$ (nN/nm)
Isopropanol/neutral	0.35±0.03	32±3	0.37±0.04	31±4	0.39±0.05	23±5	0.40±0.03	18±3
0.1 M $NaClO_4$/neutral	0.38±0.03	30±4	0.39±0.05	35±6	–	–	–	–
Isopropanol/chemically oxidized	0.36±0.04	34±3	0.41±0.05	35±6	0.63±0.05	27±5	0.40±0.02	19±4
0.1 M $NaClO_4$/EC oxidized	0.65±0.05	45±8	0.63±0.04	39±6	–	–	–	–
THF/neutral data Shi et al.[a]	–	–	0.41±0.01	53.0±1.0	–	–	–	–
THF/chemically oxidized data Shi et al.[a]	–	–	0.46±0.01	115.0±1.0	–	–	–	–

[a] Data taken from Ref. [34].

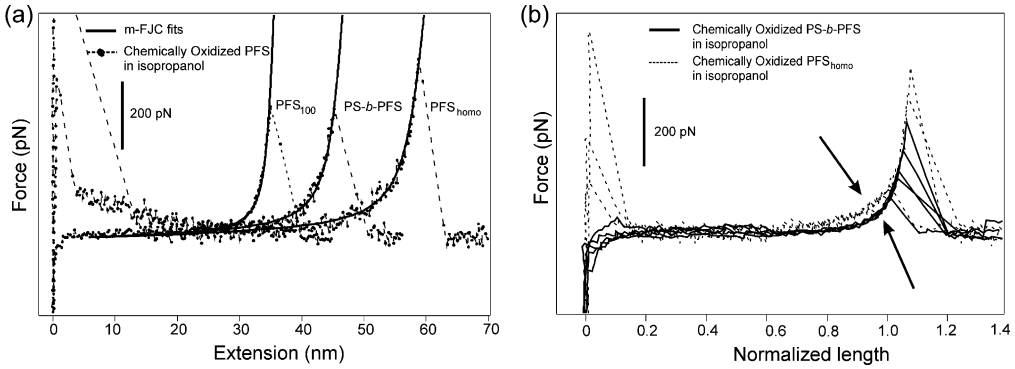

Fig. 3. (a) Force–extension curves of individual chemically oxidized PFS_{100}, PFS_{homo} and PS-*b*-PFS chains stretched in isopropanol with superimposed m-FJC fits (shown as solid lines). (b) Superposition of normalized force curves for PFS_{homo} (dotted lines) and PS-*b*-PFS (solid lines). The arrows point at different elasticity behavior between PFS_{homo} and PS-*b*-PFS.

almost identical Kuhn lengths ($\sim$0.40 nm) and $K_{segment}$ values ($\sim$35 nN/nm) were determined for PFS_{100} and PFS_{homo}. These data are also to within the experimental error identical to those of the neutral PFS. For PS-*b*-PFS chains, m-FJC fits yielded an increased Kuhn length of 0.63 ± 0.05 nm and $K_{segment}$ values of 27 ± 5 nN/nm, which are clearly different from the PFS homopolymers.

The observations of unaltered elasticity parameters for PFS_{100} and PFS_{homo} after the chemical oxidation process can be explained by the incomplete oxidation of the PFS homopolymer chains. This may be caused by the unfavorable solubility of the (partially) oxidized PFS. Following this interpretation, the obtained elasticities represent the properties of partially oxidized (very low degree of oxidation) or even neutral PFS homopolymer chains. By contrast, in the copolymer case, the ferrocenyl units along the chains can be oxidized to a much higher extent by the charge transfer oxidation reagent TCNE due to the better solubility of the block copolymer chains that allows the formation of $[Fe(C_5H_5)_2]^+[TCNE]^-$ [51]. The interpretation would be consistent with the observation of altered elasticities following electrochemical oxidation (see below). The elasticity of the PS block is not altered after the oxidation of PS-*b*-PFS by TCNE, as shown by the Kuhn length of 0.40 ± 0.02 nm, and $K_{segment}$ of 19 ± 4 nN/nm for PS homopolymer. These values are to within the error identical to the data obtained without TCNE treatment (Table 1).

Shi et al., who used $FeCl_3$ as chemical oxidation agent for PFS homopolymers and performed the SMFS experiments in THF [34], reported a substantial increase in the enthalpic elasticity for PFS_{homo}. The Kuhn length increased by 10% following oxidation, while the segment elasticity was more than doubled (Table 1). These data indicate, in agreement with our data, that the elasticity of individual PFS macromolecules was changed after oxidation.

3.4. Electrochemically oxidized PFS macromolecules

A central requirement for a molecular motor is the possibility to repeatedly/continuously run a cycle in a reversible manner (or periodically) to produce work. This requirement is difficult to achieve chemically. Reversible electrochemical oxidation and reduction are much more promising, as discussed in Section 1. Therefore, the elasticity of electrochemically oxidized PFS_{100} and PFS_{homo} were studied by SMFS using the AFM set-up equipped with an external potentiostat.

The electrochemical responses of PFS_{100} and PFS_{homo} were determined using CV in the electrochemical SMFS measurement configuration. Fig. 4 shows the CV data recorded in 0.1 M $NaClO_4$ aqueous solution (in situ in the AFM liquid cell), in which the reversible redox behavior for the PFS polymers is clearly recognized. The oxidation and reduction potentials were obtained using a Pt reference electrode (instead of $Hg/HgSO_4$ used, e.g. in Ref. [44]); hence the values have shifted to more positive potentials compared to the CV data reported before [44–46].

The cyclic voltammograms indicate that PFS homopolymer chains can be reversibly oxidized and reduced by applying an external potential. The voltammogram of PFS_{100} (shown in Fig. 4, thin line) was recorded on neat PFS_{100} layers prepared from toluene solution to increase the electrochemical redox signal. The surface coverages of different PFS polymer chains

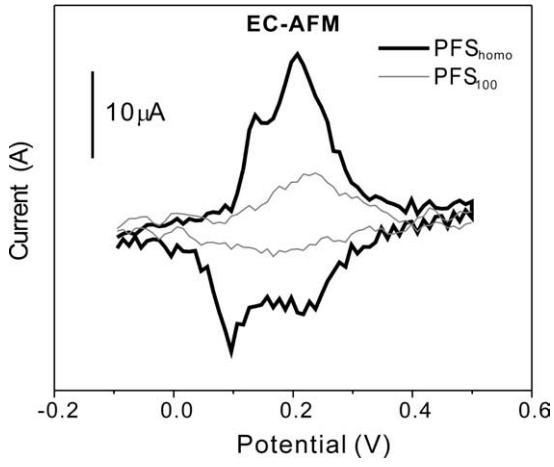

Fig. 4. Cyclic voltammograms of 7 ± 2 nm thick PFS_{homo} layer (thick line) and PFS_{100} layer self-assembled from 4 ± 10^{-7} M toluene solution (thin line) on gold substrates recorded in the electrochemical SMFS set-up (scan rate $v =$ 50 mV/s, electrolyte: 0.1 M $NaClO_4$, working electrode: Au substrate; reference and counter electrode: Pt).

were estimated according to Ref. [44]. The integrated charge transfer was $\sim 1.8\times10^{-5}$ C for PFS_{100}, as calculated from the CV plot. The surface coverage of ferrocenyl sites (Γ_{Fc}) was determined based on the transferred charge over the electrode area according to Eq. (1)

$$\Gamma_{Fc} = \frac{Q_{Fc}}{nFA} \quad (1)$$

where n is the number of electrons involved in the electron transfer process ($n=1$), F is the Faraday constant and A is the geometric surface area of the electrode ($A=0.35$ cm^2).

The number of PFS_{100} chains per unit area (Γ) was calculated by dividing Γ_{Fc} to the degree of polymerization (DP, 92 for PFS_{100}), which yielded a value of $\Gamma=3.2\times10^{-2}$ chains/nm^2. Following the same procedure, the integrated charge transfer for PFS_{homo} was obtained as $\sim 4.9\times10^{-5}$ C. The calculated surface coverage of PFS_{homo} chains gave the value of $\Gamma=3.0\times10^{-2}$ chains/nm^2.

To estimate the elasticity of completely oxidized PFS macromolecules, samples with PFS_{100} and PFS_{homo} chains were subjected to the SMFS measurements under a constant external potential of $+0.5$ V. The force–extension curves of electrochemically oxidized PFS molecules are presented in Fig. 5 together with fits to the m-FJC model.

We observed for both systems a significant increase in Kuhn length compared to the neutral state (Table 1). The trend of the elasticity parameters upon oxidation is qualitatively similar to the trend observed for the chemically oxidized block copolymer, i.e. the segment elasticities, and in particular the Kuhn lengths, increase.

The clearly different elastic properties of oxidized PFS molecules compared to the neutral PFS homopolymers, as determined by means of SMFS after electrochemical oxidation, show that control of the elasticity by changing from oxidized PFS to neutral PFS reversibly, and thereby a single molecule motor based on PFS, can in principle be realized.

3.5. Changes of the elasticity of PFS between the neutral and oxidized states

The observed increased Kuhn length (length from of ~ 0.40 nm in the neutral state to ~ 0.65 nm in the oxidized state) of the PFS molecules after oxidation can be explained by an additional electrostatic contribution. This contribution originates from the positive charges that are distributed along the polymer chains. According to the classical Odijk–Skolnick–Fixman (OSF) theory [54,55], it is expected that the electrostatic interactions between the charges along the polymer chain increase the distances between like-charged segments, i.e. the stretched conformation of the chains is favored. The resulting increase in Kuhn length corresponds to a lower restoring force or elasticity of the oxidized PFS.

As pointed out above, the elasticity of PS-*b*-PFS filaments may include a contribution from PS blocks (which itself is identical for the neutral and the oxidized states). This

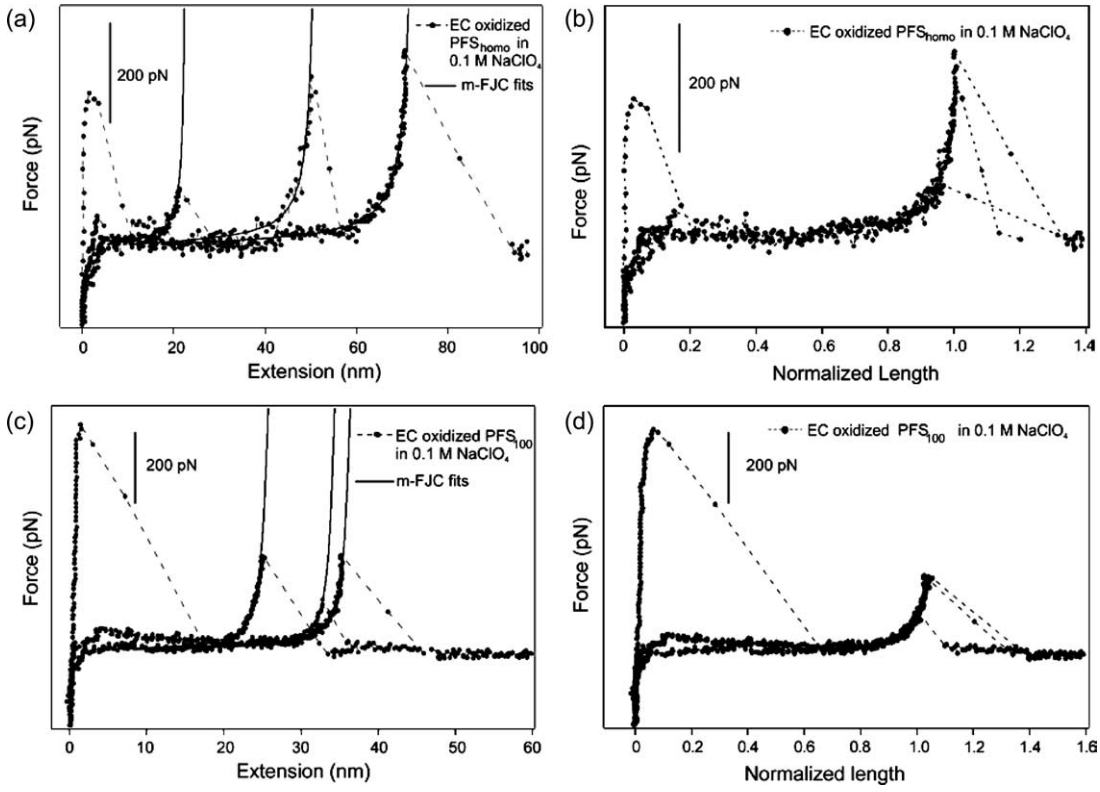

Fig. 5. (a) Typical force–extension curves of electrochemically oxidized PFS_{homo} superimposed with m-FJC fits (solid lines); (b) superposition of normalized force curves for oxidized PFS_{homo}; (c) force–extension curves of electrochemically oxidized PFS_{100} superimposed with m-FJC fits (solid lines); (d) superposition of normalized force curves for oxidized PFS_{100}. Panels (c) and (d) reproduced from Ref. [36] with permission from Wiley–VCH.

contribution can be estimated as 27% [56]. The changes of elasticity induced either by chemical or electrochemical stimuli offer the possibility for realizing the ultimate target: a simple mechanical molecular motor based on controlling the elasticity.

3.6. Chemically and electrochemically induced mechanical work

As explained in the introduction, the output or the work of a thermal cycle W_{out} is the mechanical energy converted from the transferred heat. For the molecular motor using a single polymer chain as working substance (Fig. 6(a)), the mechanical work (output) of the cycle corresponds to the effectively converted electrochemical potential.

One possible experimental cycle to realize the molecular motor is shown in Fig. 6, which is defined by keeping the deflection of the cantilever constant in SMFS measurements, i.e. constant force, during the transition from the oxidized state to the neutral state (vice versa) [57]. The two branches are determined by the elasticities of the polymer, which are well described by the m-FJC model in the low force range.

As shown in Fig. 6(b), starting from a force of 20 pN (point 1) under an applied constant external potential of +0.5 V, an individual, oxidized PFS polymer chain of 50 nm contour length is pulled to a force of 140 pN (point 2). At a constant force of 140 pN, the PFS chain is reduced to its neutral state by controlling the external potential back to 0 V (point 3), resulting in a change of the elasticity of the polymer chain. Then the force on the polymer is reduced back to 20 pN (point 4). Finally, the cycle is completed by applying the external potential of +0.5 V in order to completely oxidize the whole PFS chain. By periodically controlling the external potential, the corresponding oxidized and/or neutral PFS chains can be created to realize the operating cycle. The mechanical work performed by the PFS polymer chain of 3.4×10^{-19} J can be calculated as the integrated area of the cycle shown in Fig. 6.

3.7. Efficiency of converting electrochemical energy to mechanical work

The efficiency of the cycle shown in Fig. 6 can be estimated according to Eq. (2) based on the assumption that all electrons (80 electrons pet chain in Fig. 6) [58] reach the PFS chain

$$\eta = \frac{W_{out}}{\Delta\mu\Delta N} \tag{2}$$

where, W_{out} is the mechanical work, $\Delta\mu$ is the change of the electrochemical potential and ΔN is the number of transferred charges during the oxidation/reduction processes.

Assuming that each ferrocenyl group has been oxidized to ferrocenium and each unit bears one charge, the change of electrochemical potential is estimated as

$$\Delta\mu = \bar{\mu}_i - \mu_i = z_i F \Delta\phi \tag{3}$$

here $\bar{\mu}_i$ represents the chemical potential of the electrochemically oxidized PFS chain (also called electrochemical potential), μ_i is the chemical potential of the neutral PFS chain, z_i is number of charges per redox center ($z_i=1$), F is the Faraday constant (96,486 C/mol) and $\Delta\phi$ is the electric potential to complete the oxidation of the entire PFS chain.

Consequently, an energy of $\sim6.4\times10^{-18}$ J is needed under the externally applied potential (0.5 V) to complete one cycle. With the total mechanical work of 3.4×10^{-19} J (estimated from the area of the cycle), an efficiency of ~5% is obtained for this simple electrochemical mechanical motor.

For their optomechanical single molecule cycle Hugel et al. reported a maximum efficiency η of ~10% [22]. For PFS, a potential difference of 0.5 V was used to ensure the complete oxidation of the entire polymer chain on the Au electrodes. However, if an individual polymer chain close to the electrode surface can be addressed, the external potential difference could be reduced to 0.25 V, which obviously would increase the efficiency to ~10% (approaching the same value reported by Hugel et al.) [22].

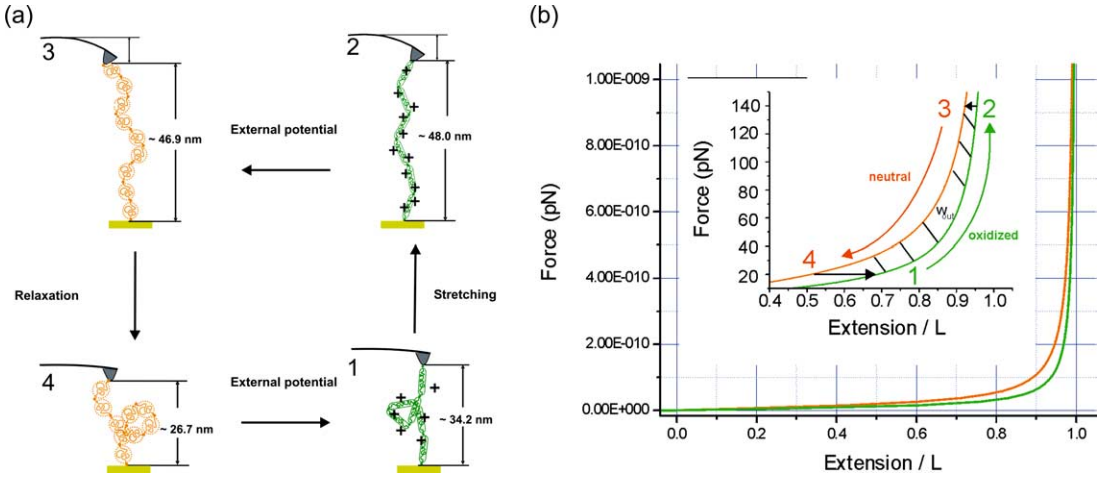

Fig. 6. (a) Schematic illustration of a single molecule operating cycle with redox-active macromolecules. (b) Single molecule operating cycle of PFS macromolecules (DP = 80) powered by an electrochemical potential calculated based on the SMFS experimental data. Force curves (force vs. normalized extension) were plotted based on the m-FJC function with Kuhn lengths of 0.40 nm (neutral PFS) and 0.65 nm (oxidized PFS), and segment elasticities of 30 nN/nm (neutral PFS), and 45 nN/nm (oxidized PFS).

The analysis of the dependence of W_{out} on chain length showed in a first approximation a direct proportionality. As the electrochemical energy for oxidation and reduction is also proportional to the number of charges passed to/from the polymer chain (compare Eq. (2)), the overall efficiency remains virtually unchanged.

The simplified estimate of the efficiency shown above does not explicitly take the contribution of the counter ions, nor possible energy dissipation into account. Since the efficiency (for one molecule with a constant number of redox active centers) is directly related to the work (W_{out}), which in turn is related to the elasticity difference between the two states, the efficiency can potentially be increased by enhancing the relative change of elasticity upon oxidation/reduction.

4. Conclusions

We have shown that external chemical or electrochemical stimuli can be used to induce reversible elasticity changes of individual PFS chains on surfaces by changing the redox state between neutral and oxidized. The changes were assessed at the single molecule level by SMFS. PFS homopolymers were found to be at most only partially oxidized by TCNE as chemical oxidant, while block copolymers could be oxidized successfully. Using the m-FJC model to fit the force–extension data measured on single PFS chains, an increased Kuhn length of $\sim$0.65 nm and a segment elasticity of $\sim$45 nN/nm were obtained for oxidized PFS compared to a Kuhn length of $\sim$0.40 nm and a segment elasticity of $\sim$30 nN/nm for neutral PFS. The detected changes of the elasticity of individual chemical/electrochemical-stimuli-responsive PFS chains are the basis for the demonstration of the principle of a single (macro)molecular motor. For PFS homopolymers with DP$\sim$80 a work of $\sim 3.4\times10^{-19}$ J and an efficiency of 5% were estimated based on the experimental data.

Acknowledgements

The authors acknowledge Dr M. Péter and Dr R.G.H. Lammertink for their contribution in the synthesis of PFS_{100}. This work has been supported by the MESA$^+$ Institute for Nanotechnology (MESA$^+$ Strategic Research Orientation Nanolink) of the University of Twente.

References

[1] Wang HY, Oster G. Nature 1998;396:279–82.
[2] Keller D, Bustamante C. Biophys J 2000;78:541–56.
[3] Bustamante C, Keller D, Oster G. Acc Chem Res 2001;34:412–20.
[4] Vale RD, Milligan RA. Science 2000;288:88–95.
[5] Rayment I, Holden HM, Whittaker M, Yohn CB, Lorenz M, Holmes KC, et al. Science 1993;261:58–65.
[6] Atsumi T, McCarter L, Imae Y. Nature 1992;355:182–4.
[7] Molecular motors may be defined as follows: a molecule is operated in a controlled cyclic fashion to perform mechanical movement (output) as a consequence of appropriate external stimulation (input). During the operating process, a number of steps are executed, which correspond to changes in conformation and/or in chemical state of the molecules. Eventually the molecules are reset to the initial conformation. The steps of the mechanical cycle are coupled to the states of a chemical cycle (stimulated by light, electric or other possible fuels) that generates the energy necessary to fuel the movement.
[8] Balzani V, Credi A, Raymo FM, Stoddart JF. Angew Chem Int Ed 2000; 39:3349–91.
[9] Feringa BL. Acc Chem Res 2000;33:346–53.
[10] Collin JP, Dietrich-Buchecker C, Gavina P, Jimenez-Molero MC, Sauvage JP. Acc Chem Res 2001;34:477–87.
[11] Pease AR, Jeppesen JO, Stoddart JF, Luo Y, Collier CP, Heath JR. Acc Chem Res 2001;34:433–44.
[12] Schalley CA, Beizai K, Vogtle F. Acc Chem Res 2001;34:465–76.
[13] Balzani V, Credi A, Venturi M. Proc Nat Acad Sci USA 2002;99:4814–7.
[14] Atkins PW. Physical chemistry. 6th ed. Oxford: Oxford University Press; 1998 p. 102.
[15] Steinberg IZO, Katchalsky A. Nature 1966;210:568–71.
[16] Steinberg et al. have pointed out that a collagen tape can be used for this purpose [15]. Such a tape contains a triple helix conformation, oriented in the direction of the fiber and tape axis. Upon exposure to a concentrated salt solution (e.g. 5 M LiBr), the triple helix is not stable and denatures into a random-coil state, where the molecular dimensions are much smaller. As a result the whole tape contracts. Upon removal of the salt or lowering its concentration (e.g. 2.5 M LiBr), the collagen renatures to the oriented triple helix form. Consequently, the tape lengthens again.
[17] Pines E, Wun KL, Prins W. J Chem Educ 1973;50:753–6.
[18] Baughman RH. Synth Met 1996;78:339.
[19] Smela E, Inganäs O, Lundström I. Science 1995;268:1735.
[20] Kaneto K, Kaneko M, Min Y, MacDiarmid AG. Synth Met 1996;78:339.
[21] Baughman RH, Cui C, Zakhidov AA, Iqbal Z, Barisci JN, Spinks GM, et al. Science 1999;284:1340.
[22] Hugel T, Holland NB, Cattani A, Moroder L, Seitz M, Gaub HE. Science 2002;296:1103–6.
[23] Hugel T, Seitz M. Macromol Rapid Commun 2001;22:989–1016.
[24] Janshoff A, Neitzert M, Oberdorfer Y, Fuchs H. Angew Chem Int Ed 2000;39:3213–37.
[25] Zhang W, Zhang X. Prog Polym Sci 2003;28:1271–95.
[26] Ludwig M, Rief M, Schmidt L, Li H, Oesterhelt F, Gautel M, et al. Appl Phys A: Mater Sci Process 1999;68:173–6.
[27] Rief M, Oesterhelt F, Heymann B, Gaub HE. Science 1997;275:1295–7.
[28] Li HB, Rief M, Oesterhelt F, Gaub HE, Zhang X, Shen JC. Chem Phys Lett 1999;305:197–201.
[29] Marszalek PE, Oberhauser AF, Pang YP, Fernandez JM. Nature 1998; 396:661–4.
[30] Oberhauser AF, Hansma PK, Carrion-Vazquez M, Fernandez JM. Proc Nat Acad Sci USA 2001;98:468–72.
[31] Schönherr H, Beulen MWJ, Bügler J, Huskens J, van Veggel F, Reinhoudt DN, et al. J Am Chem Soc 2000;122:4963–7.
[32] Zou S, Schönherr H, Vancso GJ. Angew Chem Int Ed 2005;44:956–9.
[33] Melosh NA, Boukai A, Diana F, Gerardot B, Badolato A, Petroff PM, et al. Science 2003;300:112–5.
[34] Shi WQ, Cui S, Wang C, Wang L, Zhang X, Wang XJ, et al. Macromolecules 2004;37:1839–42.
[35] Zou S. PhD thesis, University of Twente: Enschede, The Netherlands; 2005.
[36] Zou S, Hempenius MA, Schönherr H, Vancso GJ. Macromol Rapid Commun; 2006; 27:103–8.
[37] Ryan AJ, Crook CJ, Howse JR, Topham P, Jones RAL, Geoghegan M, et al. Faraday Discuss 2005;128:55–74.
[38] Kulbaba K, Manners I. Macromol Rapid Commun 2001;22:711–24.
[39] Foucher DA, Ziembinski R, Tang BZ, Macdonald PM, Massey J, Jaeger CR, et al. Macromolecules 1993;26:2878–84.
[40] Nguyen MT, Diaz AF, Dement'ev VV, Pannell KH. Chem Mater 1993;5: 1389–94.
[41] Pudelski JK, Foucher DA, Honeyman CH, Macdonald PM, Manners I, Barlow S, et al. Macromolecules 1996;29:1894–903.
[42] Foucher DA, Ziembinski R, Petersen R, Pudelski J, Edwards M, Ni YZ, et al. Macromolecules 1994;27:3992–9.
[43] Péter M, Hempenius MA, Lammertink RGH, Vancso GJ. Macromol Symp 2001;167:285–96.

[44] Zou S, Ma Y, Hempenius MA, Schönherr H, Vancso GJ. Langmuir 2004; 20:6278–87.
[45] Péter M, Lammertink RGH, Hempenius MA, van Os M, Beulen MWJ, Reinhoudt DN, et al. Chem Commun 1999;359–60.
[46] Péter M, Hempenius MA, Kooij ES, Jenkins ATA, Roser SJ, Knoll W, et al. Langmuir 2004;20:891–7.
[47] Schönherr H, Vancso GJ, Huisman B-H, van Veggel FCJM, Reinhoudt DN. Langmuir 1999;15:5541–6.
[48] Florin EL, Rief M, Lehmann H, Ludwig M, Dornmair C, Moy VT, et al. Biosens Bioelectron 1995;10:895–901.
[49] Butt HJ, Jaschke M. Nanotechnology 1995;6:1–7.
[50] Nguyen MT, Diaz AF, Dement'ev VV, Pannell KH. Chem Mater 1994;6: 952–4.
[51] Hempenius MA. Unpublished data.
[52] The FJC model, which is applicable for small extensions, solely considers entropic effects. For large extensions, before the chain may rupture (chemical bonds break), the deformation of bond angles and the stretching of covalent bonds will result in an effective increase in the segment length. For larger extensions (for $x = L$), the simple FJC model thus fails to describe the stretching of the macromolecules. Therefore, enthalpic contributions to the restoring force of the polymer chain must be considered. The simplest way to solve this problem is to separate the restoring force into an entropic and an enthalpic contribution such that the extensibility of the segments can be considered as an additional Hookean term (modified FJC model).
[53] The frequency of observed stretching events was around 1% for all of the three polymers.
[54] Odijk T. Macromolecules 1979;12:688–93.
[55] Skolnick J, Fixman M. Macromolecules 1977;10:944–8.
[56] The calculation was performed by calculating a weighted average of L(PS-*b*-PFS): $L(\text{PS-}b\text{-PFS}) = xL(\text{PS}) + (1-x)L(\text{PFS})$, where L is the modified Langevin function and x is the fraction of PS block in the copolymer chain. This function was fitted to the force–extension curve of oxidized PS-*b*-PFS with a Kuhn length of 0.63 nm and a K_{segment} of 27 nN/nm. This procedure yielded the result of $x = 27\%$.
[57] One can also define the cycle with constant piezo extension during the oxidation or reduction processes, if the contraction ratio (before and after oxidation) of the polymer chain against the external force is known. In our experiments, it was not possible to measure the change of the contour length of a particular chain before and after oxidation. These data are also not reported in the literature. It is important to note that the elasticity (in terms of Kuhn length and segment elasticity) of the single polymer chain does not depend on the extension or contour lengths of the polymer, but only reflects the intrinsic properties of the polymer itself. In our experiments, it was not possible to hold the neutral polymer chain between the AFM tip and the substrate and reversibly oxidize/reduce it during force–extension measurements. However, by recording force–extension data at the very same *x*-, *y*-position both in neutral and oxidized states, it may be possible to stretch the 'same' PFS chain before and after electrochemical oxidization.
[58] A monomer repeat unit is $\sim$0.63 nm for PFS homopolymer chains and the entire PFS_{100} chain of $\sim$58 nm can be calculated by 0.63×92 (DP). So for a PFS chain with 50 nm contour length, the DP can be calculated as $50/0.63 = 80$.